Air gap assessment for floating structures in random seas

L. Manuel
Department of Civil Engineering
University of Texas at Austin, Austin, TX 78712
lmanuel@mail.utexas.edu

Abstract
First- and second-order incident and diffracted wave effects are studied to determine the influence of the motions of a semi-submersible on the instantaneous air gap. Statistics of the air gap response are estimated with different modeling assumptions. In these studies, a single field point is studied – one at the geometric center of the semi-submersible.

Next, a comparison of the air gap at different locations is studied by examining response statistics at different field points for the semi-submersible. These include locations close to columns of the four-columned semi-submersible. Analytical predictions, including first- and second-order diffracted wave effects, are compared with wave tank measurements at several locations. In particular, air gap response statistics such as the root-mean-square and the 3-hour median extreme are compared.

Background
The air gap response, and potential deck impact, of ocean structures under random waves is of considerable interest. Air gap modeling is particularly complicated in the case of floaters because of their large volume, and the resulting effects of wave diffraction and radiation. These give rise to two distinct effects: (1) global forces and resulting motions are significantly affected by diffraction effects; and (2) local wave elevation modeling can also be considerably influenced by diffraction, particularly at locations underneath the deck and/or near a major column. Both effects are important in air gap prediction: we need to know how high the waves rise (item 2 above), and how low the deck translates vertically (due to net heave and pitch) at a given point to meet the waves. Moreover, effects (1) and (2) are correlated in time, as they result from the same underlying incident wave excitation process.

We focus here on analytical diffraction models of air gap response, and its resulting stochastic nature and numerical predictions under random wave excitation. Attention is focused on a semi-submersible platform, for which both slow-drift motions (heave/pitch) and diffraction effects are potentially significant. Various effects are studied separately: e.g., wave forces on a fixed (locked-down) structure, the effect of structural motions on air gap response, and finally, the effect of different local wave elevation models in step 2. For reference, a complete second-order diffraction model is formulated and studied.

Response Statistics: Moments and Extremes
In modeling floating structures, it is common to employ Volterra series to describe the response (output) of these nonlinear systems. The nonlinear system is defined in terms of first- and second-order transfer functions. For floating structures, these transfer functions are obtained from first- and second-order wave diffraction analysis programs such as WAMIT (e.g., WAMIT, 1995).

We start by defining a sea surface elevation, $\eta(t)$, in terms of a sum of sinusoidal components at N distinct frequencies and a wave spectrum, $S_\eta(\omega)$ as follows:

$$\eta(t) = \sum_{k=1}^{N} a_k \cos(\omega_k t + \theta_k) = \text{Re} \sum_{k=1}^{N} A_k \exp(i\omega_k t); \quad A_k = \sqrt{2S_\eta(\omega_k)\Delta\omega} \exp(i\theta_k) \qquad (1)$$

Any response quantity, $x(t)$, may then be described by a second-order Volterra series representation as follows:

$$x(t) = x_1(t) + x_2(t) = x_1(t) + x_{2-}(t) + x_{2+}(t) \tag{2}$$

where $x_1(t)$, $x_{2-}(t)$, and $x_{2+}(t)$ are the first-order, second-order difference-frequency and second-order sum-frequency contributions, respectively, to the response. We can write each of these components in terms of transfer functions. Thus, we have:

$$x_1(t) = \text{Re} \sum_{k=1}^{N} A_k H_k^{(1)} \exp(i\omega_k t)$$

$$x_{2\pm}(t) = \text{Re} \sum_{k=1}^{N} \sum_{l=1}^{N} A_k A_l^{\pm} H_{kl}^{(2\pm)} \exp[i(\omega_k \pm \omega_l)t]; \quad A_l^+ = A_l; \quad A_l^- = A_l^* \tag{3}$$

We will characterize the physical response model and estimate response extremes using the first four statistical moments of the response. One can then express $x(t)$ in terms of mutually independent standard Gaussian processes, $u_j(t)$. Thus, we have:

$$x_1(t) = \sum_{j=1}^{2N} c_j u_j(t); \quad x_2(t) = \sum_{j=1}^{2N} \lambda_j u_j^2(t) \tag{4}$$

The coefficients c_j and λ_j are obtained by solving an eigenvalue problem involving the transfer functions and input power spectral densities (see Kac and Seigert, 1947). To represent the four statistical moments, we will employ the mean (m_x), standard deviation (σ_x), and the dimensionless coefficients of skewness (α_{3x}) and kurtosis (α_{4x}):

$$m_x = E[x(t)]; \quad \sigma_x^2 = E[(x(t) - m_x)^2]$$

$$\alpha_{3x} = E[(x(t) - m_x)^3] / \sigma_x^3; \quad \alpha_{4x} = E[(x(t) - m_x)^4] / \sigma_x^4 \tag{5}$$

In terms of c_j and λ_j, these first four moments may be given as follows:

$$m_x = \sum_{j=1}^{2N} \lambda_j; \quad \sigma_x^2 = \sum_{j=1}^{2N} (c_j^2 + \lambda_j^2)$$

$$\alpha_{3x} = \frac{1}{\sigma_x^3} \sum_{j=1}^{2N} (6c_j^2 \lambda_j + 8\lambda_j^3); \quad \alpha_{4x} = 3 + \frac{1}{\sigma_x^4} \sum_{j=1}^{2N} (48c_j^2 \lambda_j^2 + 48\lambda_j^4) \tag{6}$$

Once these moments are found, the response process $x(t)$ may be related to a standard Gaussian process $u(t)$ using a Hermite transformation model (Winterstein, 1998):

$$x = m_x + \kappa \sigma_x [u + c_3(u^2 - 1) + c_4(u^3 - 3u)] \tag{7}$$

where c_3, c_4 and κ are coefficients that can be estimated in terms of α_{3x} and α_{4x}.

The p-fractile extreme response in a seastate duration T can then be estimated from Eq. (7) taking u as the corresponding Gaussian p-fractile extreme:

$$u_{\max, p} = [2\ln(\frac{v_0 T}{\ln(1/p)})]^{1/2} \tag{8}$$

where v_0 is the average response frequency.

Air Gap Response

We start by defining the net wave elevation, η_{NET}, with respect to a fixed origin. Then, if at a field point of interest, (x,y), $\delta(t)$ denotes the net vertical displacement of the structure, the relative wave elevation $r(t)$ measured with respect to the moving structure may be given by:

$$r(t) = \eta_{NET}(t) - \delta(t); \quad \text{where} \quad \delta(t) = \xi_3(t) + y \cdot \xi_4(t) - x \cdot \xi_5(t) \tag{9}$$

implying that $\delta(t)$ is given in terms of the heave (ξ_3), roll (ξ_4), and pitch ((ξ_5), motions. The available air gap $a(t)$ is the difference between the still-water air gap and $r(t)$:

$$a(t) = a_0(t) - r(t) \tag{10}$$

The instantaneous net wave elevation, $\eta_{NET}(t)$, in Eq. (9) is a result of both the incident waves that would occur if the structure were not present, and the diffracted waves that arise because of the presence of the structure that alters the flow field.

$$\eta_{NET}(t) = \eta_{1,NET}(t) + \eta_{2,NET}(t)$$

$$\eta_{1,NET}(t) = \eta_{1,I}(t) + \eta_{1,D}(t); \quad \eta_{2,NET}(t) = \eta_{2,I}(t) + \eta_{2,D}(t)$$

$$(11)$$

In Eq. (11), we see that in our second-order model, we need to represent the net wave elevation as made up of first- and second-order effects due to both incident and diffracted waves. The first-order incident wave $\eta_{1,I}$ is modeled as a stationary Gaussian process, and consistent values of $\eta_{1,D}$, $\eta_{2,I}$, and $\eta_{2,D}$ are calculated from hydrodynamic theory.

The methodology using Volterra series models and moment-based extreme estimation has been implemented in a post-processing routine (Ude et al., 1996) that uses first- and second-order *force* transfer functions and added mass and damping. The transfer functions combined with stiffness, damping, and inertia properties of the structure provide first- and second-order transfer functions to any response quantity, *x(t)*.

In computing the air gap response, we need to simultaneously include both second-order sum-frequency effects (on the wave surface), and second-order difference-frequency effects (on slow drift motions). The air gap response, as described by Eqs. (9) through (11) above, has been implemented in the formulation based on second-order Volterra series and moment-based extremes models (Manuel and Winterstein, 1998).

Platform Description
The structure chosen for the numerical studies is the Troll semi-submersible. Figure 1 shows a plan view of the platform that has four columns and plan dimensions, 100m x 100m. The still-water air gap is 25 meters and the mean water depth is 325 meters. Measurements of air gap were made at seven different field point locations. At these same locations, WAMIT diffraction analyses were performed for waves with different headings and with wave periods ranging from 7.4 to 20.0 seconds. The seven field points' locations are indicated on Figure 1.

Alternative Modeling Options
We are interested in studying the influence of alternative modeling options in describing the relative wave. We will study the air gap at field point no. 1 and will consider a 3-hour seastate characterized by head seas and with a significant wave height of 10.6 meters and a spectral peak period of 12.5 seconds.

To isolate the effects of incident and diffracted waves of first- and second-order, and the effect of net vertical motion, we consider several different cases. Table 1 summarizes the response statistics for the Troll submersible in each of the cases defined. Contributions to the response statistics from the first-order effects alone and from the sum of first- and second-order contributions are included. From the table, the following findings may be noted as we move across the various cases:

Case 0 *Only first-order incident waves ($\eta_{1,I}$) included; structure locked down (i.e., motions prevented, $\delta = 0$).* Because this case includes only first-order incident waves, the net wave elevation is seen to be Gaussian. Also, the rms response (2.65 meters) is equal to one-fourth of the significant wave height (10.6 meters). The Gaussian character is also confirmed by the peak factor on the median extreme of 3.8 (see Eq. 3.8 with $p = 0.5$, $\nu_0 T = 1080$) as expected for a 3-hour seastate.

Case 1 *Only first- and second-order incident waves ($\eta_{1,I}$ and $\eta_{2,I}$) included; structure locked down.* Case 1 includes a second-order Stokes incident wave process, which causes the net wave elevation to be non-Gaussian and positively skewed. The second-order process provides a small contribution to the total response: its rms is only 14% of that of the first-order process. The peak factor of the total process is 4.1.

Case 2 *First-order incident and diffracted waves ($\eta_{1,I}$ and $\eta_{1,D}$), second-order incident waves ($\eta_{2,I}$) included; structure locked down.* Addition of the first-order diffracted waves in Case 2 has the effect of raising the rms of the first-order process by 23% and the median extreme by 20%. The peak factor of the total process response is 3.7 (i.e., the total process is more Gaussian than in Case 1 due to the larger relative contribution of the first-order effects).

Case 3 *First- and second-order incident and diffracted waves ($\eta_{1,I}$, $\eta_{1,D}$, $\eta_{2,I}$, and $\eta_{2,D}$) included; structure locked down.* Addition of second-order diffracted waves in Case 3 causes a large increase in response, most notably in its extreme levels. In particular, the rms level changes only from 3.27m to 3.50m, while the peak factor grows from 3.7 to 5.5. This enhanced peak factor is due to the marked non-Gaussian behavior predicted in this case: the skewness value is found to be 0.54, and the kurtosis value, 4.12.

Heave *Structure's heave motion (ξ_3) studied.* Again, we see that nonlinear effects (here, the effect of difference-frequency slow-drift motions) only mildly influence rms values (0.78m increases only to 0.79m), but more notably affect non-Gaussian behavior (skewness value of 0.21).

Base *First- and second-order incident and diffracted waves ($\eta_{1,I}$, $\eta_{1,D}$, $\eta_{2,I}$ and $\eta_{2,D}$) included; structure permitted to move (i.e., $\delta \neq 0$).* Finally, the base case results predict the relative wave response for a structure permitted to move. These results combine our "best" model of the wave elevation (including second-order diffraction effects as in Case 3) with our correlated model of associated vertical motions. The results show strong non-Gaussian behavior: skewness of 0.54, kurtosis of 4.55, and peak factor of 6.1. In view of their similarity with Case 3 values, these strongly non-Gaussian effects appear to be due to the presence of second-order diffracted waves, and are not weakened when structural motions are included. Of course, by permitting the structure to move with the waves, the relative wave response is reduced as compared with the locked-down structure in Case 3.

Analytical Predictions versus Wave Tank Test Data
We next compare analytical predictions with model test results. Four different seastates are considered: $(H_s, T_p) \equiv (10.6m, 12.5s)$, $(12.6m, 13.5s)$, $(13.3m, 13.0s)$, and $(14.5m, T_p = 14.0s)$. Results are shown below for three field points, including again the platform mid-point and two other locations nearer to columns.

From Table 2, we see that second-order diffraction is found to (1) only moderately increase the rms response, but (2) markedly increase peak factors and extremes. Thus, even if second-order effects in the incident wave are retained, unconservative air gap predictions may result if second-order diffraction effects are neglected. Particularly strong non-Gaussian behavior is predicted at the platform mid-point, as compared with predictions corresponding to other points nearer a column.

Finally, we compare the model predictions with the observed wave tank statistics, shown in the final two columns of Table 2. We first note that these observed extremes (peak factors) each arise from a single 3-hour test, and are therefore rather noisy estimates of the median values across many similar 3-hour conditions. Still, these results suggest that ignoring second-order diffraction effects could lead to underestimation of response extremes. When second-order diffraction effects are included, peak factors are no longer systematically underestimated but agreement with observations remains imperfect. At the platform midpoint, for instance, the predictions appear "too nonlinear." Nonetheless, these results suggest that nonlinear diffraction effects can be important, and should be studied further. We believe that the general statistical models presented here, which estimate extremes from a limited set of statistical moments, offer an efficient approach to assess the impact of various nonlinear models on extreme response levels.

Conclusions

A methodology has been presented for describing the air gap response for floating structures. The importance of incident waves relative to diffracted waves of both first and second order has been studied. For the Troll semi-submersible, a full second-order analysis (including incident and diffracted waves up to second order) is necessary; it is unconservative to neglect the second-order diffracted waves.

In comparing the different field point locations, important non-Gaussian effects are observed that differ slightly depending on the proximity to a column. The air gap at the center of the platform exhibited the greatest non-Gaussian character. This non-Gaussian character is largely a result of second-order diffracted waves.

Acknowledgements

References

1. Kac, M. and A. J. F. Seigert (1947). "On the Theory of Noise in Radio Receivers with Square Law Detectors," Journal of Applied Physics, Vol. 18, pp. 383-400.
2. Manuel, L. and S. R. Winterstein (1998). "Estimation of Air Gap Statistics for Floating Structures: Release of TFPOP Version 2.2 – A Computer Program for Performing Stochastic Response Analysis of Floating Structures," Technical Note TN-4, Reliability of Marine Structures Program, Stanford University.
3. Ude, T. C., S. Kumar, and S. R. Winterstein (1996). "TFPOP 2.1: Stochastic Response Analysis of Floating Structures under Wind, Current, and Second-Order Wave Loads," Technical Report RMS-18, Reliability of Marine Structures Program, Stanford University.
4. WAMIT, 4.0 (1995). "WAMIT: A Radiation-Diffraction Panel Program for Wave-Body Interaction – Users' Manual," Dept. of Ocean Engineering, M.I.T.
5. Winterstein, S.R. (1988). "Nonlinear Vibration Models for Extremes and Fatigue," Journal of Engineering Mechanics, ASCE, Vol. 114, No. 10, pp. 1772-1790.
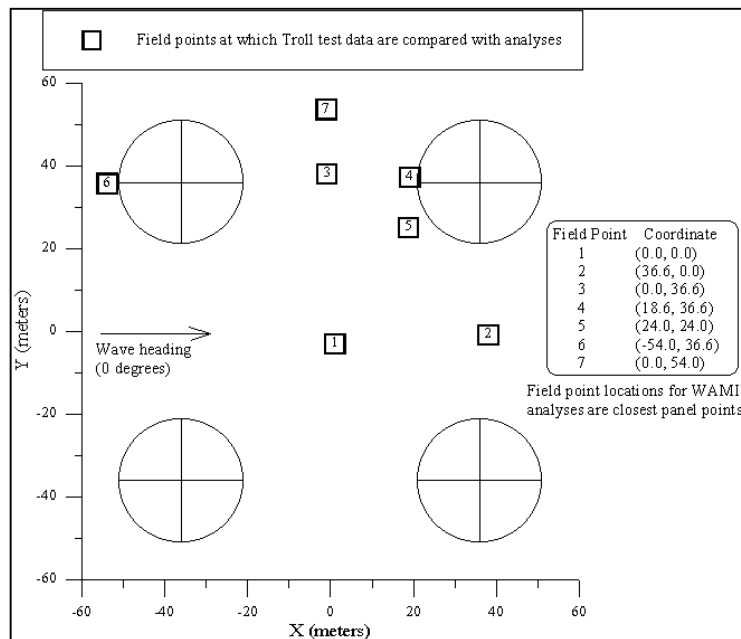
Figure 1. Plan view of Troll semi-submersible showing field points studied.

Type of Run	Response	Mean (m)	Std. Dev (m)	Skewness	Kurtosis	Median Extreme (m)	Peak Factor
Case 0	TOTAL	0.00	2.65	0.00	3.00	10.08 (-10.08)	3.8
Case 1	1st-order	0.00	2.65	0.00	3.00	10.08 (-10.08)	
	TOTAL	0.00	2.70	0.20	3.06	11.17 (-8.91)	4.1
Case 2	1st-order	0.00	3.25	0.00	3.00	12.08 (-12.08)	
	TOTAL	0.00	3.27	0.09	3.04	12.11 (-11.05)	3.7
Case 3	1st-order	0.00	3.25	0.00	3.00	12.08 (-12.08)	
	TOTAL	0.00	3.50	0.54	4.12	19.23 (-12.54)	5.5
Heave	1st-order	0.00	0.78	0.00	3.00	2.81 (-2.81)	
	TOTAL	0.07	0.79	0.21	3.13	3.34 (-2.54)	4.1
Base	**1st-order**	**0.00**	**2.52**	**0.00**	**3.00**	**9.44 (-9.44)**	
	TOTAL	**-0.07**	**2.85**	**0.50**	**4.55**	**17.18 (-12.38)**	**6.1**

Table 1 Air Gap Response Statistics for Cases involving different Modeling Options

Field Point 1 (at center)							
Hs (m)	Tp (s)	Analysis w/o 2nd-order diff. TF		Analysis w/ 2nd-order diff. TF		Wave Tank Tests	
		σ (m)	PF	σ (m)	PF	σ (m)	PF
10.6	12.5	2.55	3.7	2.85	6.0	-	-
12.6	13.5	2.96	3.8	3.37	6.2	2.78	6.5
13.3	13.0	3.19	3.8	3.71	6.4	-	-
14.5	14.0	3.34	3.8	3.89	6.4	3.20	4.3
Field Point 5 (on diagonal @ 24,24)							
Hs (m)	Tp (s)	Analysis w/o 2nd-order diff. TF		Analysis w/ 2nd-order diff. TF		Wave Tank Tests	
		σ (m)	PF	σ (m)	PF	σ (m)	PF
10.6	12.5	3.16	4.1	3.26	5.3	-	-
12.6	13.5	3.53	4.1	3.68	5.6	3.56	4.6
13.3	13.0	3.87	4.2	4.05	5.7	-	-
14.5	14.0	3.93	4.2	4.15	5.8	4.10	5.1
Field Point 6 (in front of a column)							
Hs (m)	Tp (s)	Analysis w/o 2nd-order diff. TF		Analysis w/ 2nd-order diff. TF		Wave Tank Tests	
		σ (m)	PF	σ (m)	PF	σ (m)	PF
10.6	12.5	3.62	3.7	3.66	3.7	-	-
12.6	13.5	3.78	3.7	3.85	4.1	2.69	6.3
13.3	13.0	4.29	3.7	4.37	4.0	-	-
14.5	14.0	4.13	3.8	4.24	4.4	3.17	5.7

Table 2 Response Statistics (RMS Response and Peak Factor on Median Extreme in 3 hours) – Analytical Predictions versus Wave Tank Test Data at 3 Field Points